Solvent Polarity Dependence of Photoinduced Charge Separation and Recombination Processes of Ferrocene−C_{60} Dyads

Mamoru Fujitsuka,[†] Norie Tsuboya,[‡] Ryo Hamasaki,[‡] Masateru Ito,[‡] Shinji Onodera,[†] Osamu Ito,*[,†] and Yoshinori Yamamoto*[,‡]

Institute of Multidisciplinary Research for Advanced Materials, Tohoku University, Katahira 2-1-1, Sendai 980-8577, Japan, and Department of Chemistry, Graduate School of Science, Tohoku University, Aramaki Aza Aoba, Sendai 980-8578, Japan

Received: October 3, 2002; In Final Form: December 18, 2002

Photoinduced charge-separation and charge-recombination processes of the three ferrocene−C_{60} dyads have been investigated by using laser flash photolysis methods. From molecular orbital calculations, the HOMO states are delocalized over the ferrocene and linking phenyl-ethenyl group connecting ferrocene and C_{60}, while the LUMO states are on C_{60}. From short fluorescence lifetimes ($\leq$ 120 ps) of the fullerene moieties of the dyads, charge separations were suggested. Charge-separated states in the dyads were observed upon femtosecond laser irradiation. The rate constants for the charge separation were on the order of 10^{10} s^{-1}, and the quantum yields were close to unity in various solvents, such as benzonitrile, anisole, and toluene. It was confirmed that the absorption bands of the radical cation moiety shifted to longer wavelength side in polar solvents, probably due to structural change in the charge-separated states. The lifetimes of the charge-separated states of the dyads with longer linkage became longer, up to several 10s of nanoseconds in less polar solvents, while the lifetimes in polar solvents were shorter, since the charge-recombination processes are in the Marcus "inverted region". On the other hand, the lifetime of the charge-separated state in the dyad with an acetyl linking group was on the order of nanoseconds in all of the solvents because of fast charge recombination of shorter distance. It was confirmed that the charge-recombination process generated the ground state of the dyads predominantly.

Introduction

Recently, functionalizations of fullerenes with donor molecules have been carried out by several groups.[1−7] For fullerene molecules linked with donor, fast charge separation and slow charge recombination have been reported.[4c] As for donors of the dyad molecules, aromatic amino compounds,[2] carotenoid,[3] porphyrins,[4] tetrathiafulvalenes,[5] oligothiophenes,[6] ferrocene,[7,8] and so on[9,10] have been employed. In some dyad systems, the ratios of the charge-separation rate to the recombination rate are reported to be as large as 10^4-10^5.[4g,9f,10] These fullerene-donor linked molecules on the electrode exhibit excellent photovoltaic effects upon photoirradiation.[4d,6d] These interesting properties can be attributed to high efficiency of the charge-separation process and stability of the charge-separated states in the fullerene−donor linked molecules.[1−10]

Ferrocene derivatives are electron donors with considerably low oxidation potentials. Several research groups employed ferrocene derivatives as donor groups of the donor−fullerene dyads and triads.[7,8] In the series of studies by Prato et al., they showed distance dependence of the photoinduced charge-separation and recombination processes of ferrocene−fullerene dyads with single or double bond linkage.[7c] Furthermore, ferrocene derivatives have been employed for the multistep charge-separation systems of the triad and tetrad molecules, in which ferrocene moieties often generated the final charge-separated states due to the considerably low oxidation potentials of ferrocene derivatives.[10]

In the present report, we have studied photoinduced charge separation and recombination processes of the three kinds of novel ferrocene−fullerene dyads (Chart 1), in which ferrocene and fullerene moieties were connected by three kinds of linking groups. In the cases of **1** and **2**, acetyl-phenyl-ethenyl groups connect the ferrocene and fullerene groups, while in **3** they are connected by a simple acetyl group. Furthermore, since **1** and **2** are in the relation of cis- and trans- isomers, the conformational effect can be examined. The π-conjugation systems of the linking groups are expected to have a large effect on the properties of the donor−acceptor pairs. Additionally, the effects of structural strain around double bonds of **1** and **2** on the charge separation and recombination processes are also expected. The laser flash photolysis experiments successfully revealed these aspects of the present dyads.

Experimental Section

Materials. Syntheses of three kinds of ferrocene−C_{60} dyads (**1**, **2**, and **3** in Chart 1) were carried out in a manner similar to that described previously.[11] The procedure and spectroscopic and analytical data of **1**−**3** are described in the Supporting Information. Solvents for the spectroscopic measurements were of the best commercial grade available.

Apparatus. The subpicosecond transient absorption spectra were observed by the pump and probe method. The samples were excited with a second harmonic generation (SHG, 388 nm)

* Corresponding author.
[†] Institute of Multidisciplinary Research for Advanced Materials.
[‡] Department of Chemistry, Graduate School of Science.

10.1021/jp027122t CCC: $25.00
Published on Web 02/13/2003

CHART 1

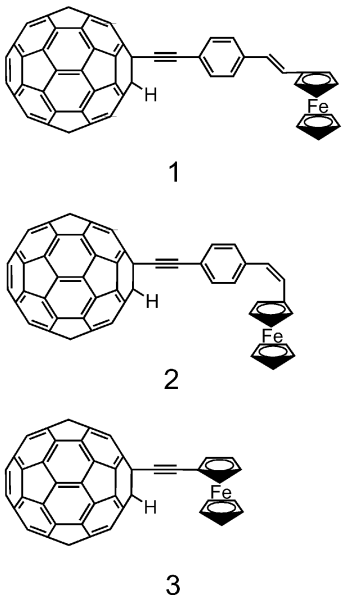

of output from a femtosecond Ti:sapphire regenerative amplifier seeded by a SHG of a Er-doped fiber laser (Clark-MXR CPA-2001 plus, 1 kHz, fwhm 150 fs). The excitation light was depolarized. A white continuum pulse generated by focusing the fundamental light on a rotating H_2O cell was used as a monitoring light. The visible monitoring light transmitted through the sample was detected with a dual MOS detector (Hamamatsu Photonics, C6140) equipped with a polychromator (Acton Research, SpectraPro 150). For detection of the near-IR light, an InGaAs linear image sensor (Hamamatsu Photonics, C5890−128) was employed as a detector. To avoid sample degradation and any nonlinear effects, a rotating cell was employed for sample. The spectra were obtained by averaging on a microcomputer.[6e]

Nanosecond transient absorption measurements were carried out using a third harmonic generation (THG, 355 nm) of a Nd:YAG laser as an excitation source. Probe light from a pulsed Xe lamp was detected with a Ge-avalanche photodiode equipped with a monochromator after passing through the sample in quartz cell (1 cm × 1 cm). Sample solutions were deaerated by bubbling Ar gas through the solutions for 15 min. Details of the transient absorption measurements were described in our previous papers.[6b,c,e,9f,h]

Steady-state absorption spectra in the visible and near-IR regions were measured on a Jasco V570 spectrophotometer.

Fluorescence lifetimes were measured by a single-photon counting method using a streakscope (Hamamatsu Photonics, C4334−01). The samples were excited with SHG (410 nm) of a Ti:sapphire laser (Spectra-Physics, Tsunami 3950-L2S, fwhm 130 fs) equipped with a pulse selector (Spectra-Physics, 3980) and a harmonic generator (Spectra-Physics, GWU-23PS).

Electrochemical measurements were carried out using a BAS CV50W voltammetric analyzer.

Molecular Orbital (MO) Calculations. All calculations were made using Gaussian 98.[12] Geometry optimization and calculations of molecular orbital coefficients were performed using the Becke-style three-parameter density functional theory, using the Lee, Yang, and Parr correlation functional, with 3-21 G(*) basis set (B3LYP/3-21G(*)).[13]

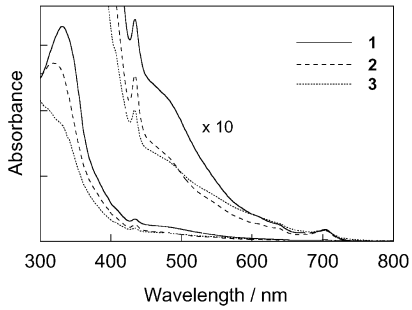

Figure 1. Absorption spectra of **1**, **2**, and **3** in toluene.

Results and Discussions

Steady-State Absorption Spectra, MO, and Redox Properties. Three dyads in the present study showed adequate solubility in various organic solvents such as toluene and benzonitrile. In toluene, **1** showed absorption bands at 703, 434, and 331 nm (Figure 1). Similarly, absorption bands were observed at 703, 434, and 319 nm for **2**, and 702, 434, and 330 nm for **3**. The absorption bands at 702−703 and 454 nm are characteristic bands of the 1,2-adduct of C_{60} derivatives, indicating that the compounds in the present study have the same C_{60} core as 1,2-adducts of C_{60}.[14] The spectral difference of **1**, **2**, and **3** seems to be large in the UV region, in which linking groups of the dyads were expected to show the absorption. Especially, larger absorbance in the 400−600 nm region of **1** indicates that the π-conjugation system of the linkage group is expanded to a great extent due to less strained structure in the comparison with **2**.

Figure 2 shows the HOMO and LUMO patterns of the present dyads calculated at B3LYP/3-21G(*) level, which has been reported to give adequate structures for dyads and triads including C_{60} and ferrocene.[8] It should be pointed out that the LUMOs of the dyads are on the C_{60} moieties, while the HOMOs are delocalized on the donor moieties including the ferrocene and the linking groups. Both the ferrocene and the linking group are expected to act as a one-donor group upon photoexcitation of each dyad. Thus, delocalization of the radical cation moiety is expected for these dyads. Ionization potentials estimated from the HOMO energy levels are in the order of **1** ≈ **2** < **3**, while the LUMO energy levels were essentially the same.

Electrochemically estimated oxidation and reduction potentials of the dyads are summarized in Table 1. Oxidation potentials are more positive in the order of **1** ≈ **2** < **3**, while the reduction potentials are essentially the same. The orders of the oxidation and reduction potentials are in the same tendency with the theoretical estimations indicating that the present results from the MO calculations are reliable. It is interesting to note that the reduction potential of pristine C_{60} is −0.54 V vs SCE, indicating that electron acceptor abilities of the C_{60} moieties of the present dyads became slightly weak. The weaker electron acceptor abilities are also reported for other functionalized fullerenes with/without the electron donor group.[15]

Fluorescence Properties of The Dyads. In toluene, **1**, **2**, and **3** showed respective fluorescence bands at 712, 713, and 718 nm upon photoexcitation at 400 nm (Figure 3). These fluorescence bands were emitted from the C_{60} moieties. In each case, fluorescence intensity is quite weak. Fluorescence quantum yields (Φ_F) for **1**, **2**, and **3** in toluene were estimated to be 7.6×10^{-5}, 8.3×10^{-5}, and 3.0×10^{-5}, respectively, by using pristine C_{60} in toluene as a standard (3.2×10^{-4}).[16] The estimated values were quite small compared with the other 1,2-adducts of C_{60} ($\Phi_F \approx 1 \times 10^{-3}$),[14] indicating that the

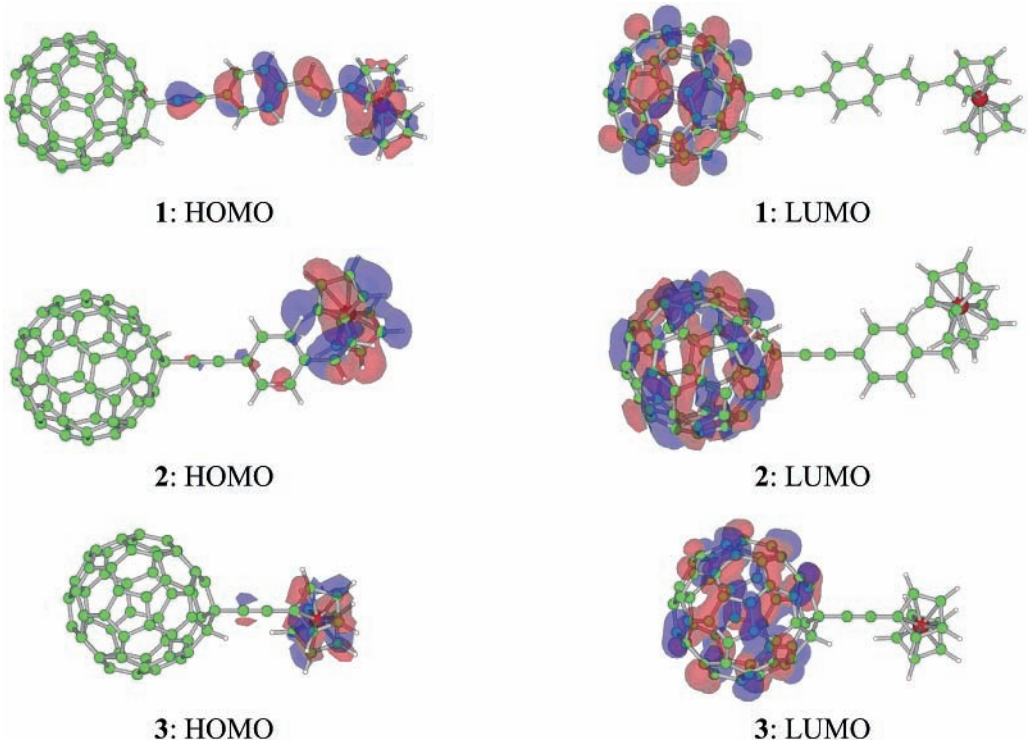

Figure 2. HOMO and LUMO patterns of **1**, **2**, and **3** calculated at the B3LYP/3-21G(*) level.

TABLE 1: Oxidation (E_{ox}) and Reduction (E_{red}) Potentials of the Ferrocene−C_{60} Dyads[a]

compound	$E_{ox}(D^{\bullet+}/D)$	$E_{red}(C_{60}/C_{60}^{\bullet-})$
1	0.50	−0.63
2	0.53	−0.64
3	0.64	−0.63

[a] All potentials were measured in *o*-dichlorobenzene including 0.1 M of tetrabutylammonium perchlorate using a SCE and platinum working and counter electrodes at 100 mV s^{-1} of scan rate.

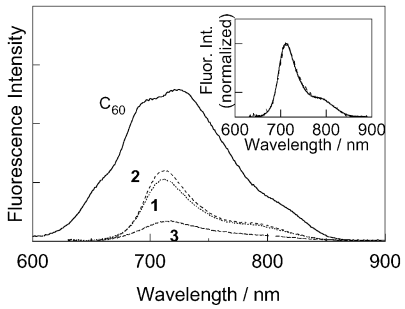

Figure 3. Fluorescence spectra of C_{60}, **1**, **2**, and **3** in toluene. Absorption intensities of the samples were matched at the excitation wavelength (400 nm). Inset: normalized fluorescence spectra of **2** in toluene (solid line) and benzonitrile (dashed line).

photoinduced processes are present in the singlet excited states of the C_{60} moieties of the present dyads. In benzonitrile, the fluorescence intensities decreased further to 1/2∼1/4 of those in toluene, while the spectra have the same shape as those in toluene (inset of Figure 3). The weak fluorescence bands of the dyads are supported by the fluorescence lifetime measurements as summarized in Table 2. The fluorescence lifetimes of **1**, **2**, and **3** are much shorter than those of pristine C_{60} and 1,2-adducts of C_{60} without electron donor (1.3 ns for each).[14] In the cases of **1** and **2**, fluorescence lifetimes became shorter in polar solvents such as anisole and benzonitrile than in nonpolar solvent. The fluorescence lifetime of **3** was shorter than the

TABLE 2: Fluorescence Lifetimes of C_{60} Moieties (τ_F), Free-Energy Changes (ΔG_{CS}), Rates (k_{CS}), and Quantum Yields (Φ_{CS}) for the Charge Separation of Ferrocene−C_{60}-Linked Compounds in Various Solvents

compound	solvent	$-\Delta G_{CS}$/eV[a]	τ_F/ps	k_{CS}/s^{-1} [b]	Φ_{CS}[b]
1	toluene	0.20	76	1.2×10^{10}	0.94
	anisole	0.64	35	2.8×10^{10}	0.97
	benzonitrile	0.86	<20	5.1×10^{10} [c]	0.98[c]
2	toluene	0.17	120	7.6×10^{9}	0.91
	anisole	0.49	42	2.3×10^{10}	0.97
	benzonitrile	0.82	<20	4.5×10^{10} [c]	0.98[c]
3	toluene	−0.04	<20	$>5 \times 10^{10}$	>0.98
	anisole	0.57	<20	$>5 \times 10^{10}$	>0.98
	benzonitrile	0.78	<20	$>5 \times 10^{10}$	>0.98

[a] Estimated by assuming that the ferrocene-ethenyl-phenyl group act as an donor for **1** and **2**. [b] From fluorescence lifetimes. [c] From transient absorption spectra.

present instrumental limitation (20 ps) in all solvents investigated in the present study. Accelerations of the decay of the singlet excited states in polar solvents strongly suggest the presence of charge-separation processes in the dyads upon photoexcitation. As summarized in Table 2, assuming that the charge separation is a predominant process in the singlet excited states of the dyads, the rate constants of the charge-separation processes (k_{CS}) were estimated from the relation: $k_{CS} = (1/\tau_{dyad}) - (1/\tau_{ref})$, where τ_{dyad} and τ_{ref} are fluorescence lifetimes of dyad and the reference compound, respectively. In the present study, the fluorescence lifetime of 1,2-adducts of C_{60} was employed as a reference (1.3 ns). Additionally, quantum yields for the charge separation (Φ_{CS}, Table 2) were calculated from the relation: $\Phi_{CS} = ((1/\tau_{dyad}) - (1/\tau_{ref}))/(1/\tau_{dyad})$. The large k_{CS} and Φ_{CS} values indicate substantial contribution of the charge-separation process to the deactivation of the singlet excited state of the fullerene moiety.

Transient Absorptions of The Dyads: Distance Dependence. To confirm the photoinduced processes of the singlet excited states of the dyads, transient absorption spectra were measured using the subpicosecond laser flash photolysis. In the

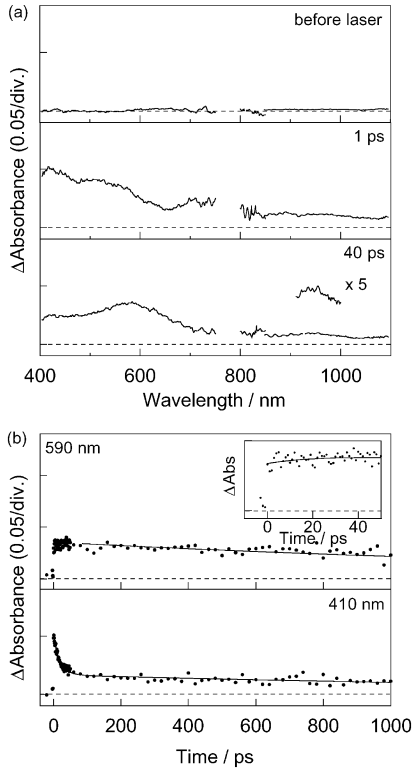

Figure 4. (a) Transient absorption spectra of **1** in benzonitrile upon excitation with femtosecond laser (388 nm, fwhm 150 fs). (b) Absorption−time profiles. Dashed lines indicate ΔAbs = 0.

case of **1** in benzonitrile, transient absorption bands appeared around 900, 550, and 450 nm immediately after the excitation at 388 nm (spectrum at 1 ps of Figure 4a). These absorption bands can be attributed to the singlet excited state of the C_{60} moiety (see Supporting Information, Figure S1). At 40 ps, new absorption bands appeared around 970 and 590 nm with a rising absorption−time profile as shown in the inset of Figure 4b. The absorption band at 970 nm can be attributed to the radical anion of the C_{60} moiety, which appeared after disappearance of singlet excited state. Furthermore, the absorption band at 590 nm will be a radical cation of the donor moiety. It has been reported that the extinction coefficient of the radical cation of ferrocene is quite small in the investigated region.[10a] In the present dyads, the linking groups that connect C_{60} and ferrocene moieties also show contributions to the HOMO as shown in Figure 2. Thus, ferrocene and the linking group seem to behave as one donor in the photoinduced processes, exhibiting the absorption band of the radical cation in the visible region. The finding indicates that the charge-separated state of **1** was generated via the singlet excited state of the C_{60} moiety as summarized in eq 1:

$$\text{Fc-sp-}C_{60} \xrightarrow{h\nu\ (388\ \text{nm})} \text{Fc-sp-}{}^1C_{60}{}^* \xrightarrow{k_{CS}} (\text{Fc-sp})^{\bullet+}\text{-}C_{60}{}^{\bullet-} \quad (1)$$

In eq 1, Fc and sp denote ferrocene and the linking group, respectively. The delocalization of the radical cation moiety has not been observed with previously reported ferrocene and fullerene dyads connected with single or double bonds.[7] The rate constant for the charge separation (k_{CS}) was estimated to be 5.1×10^{10} s^{-1} from the decay of the singlet excited state (410 nm, Figure 4b), which corresponds well with the initial rise rate of the absorption band of the radical ion pair at 590 nm (inset of Figure 4b).

The generated radical ion pair began to decay as shown in an absorption−time profile at 590 nm (Figure 4b). The decay

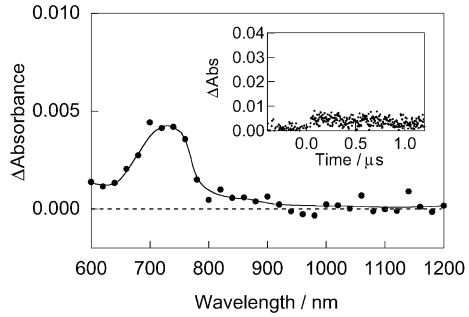

Figure 5. Transient absorption spectra of **1** in benzonitrile at 100 ns upon excitation with the nanosecond laser (355 nm, fwhm 6 ns). Dashed line indicates ΔAbs = 0. Inset: Absorption−time profile at 700 nm.

SCHEME 1

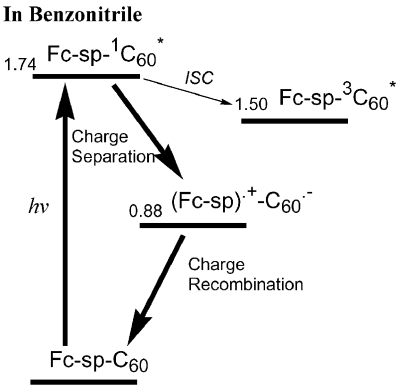

can be attributed to the charge recombination (eq 2):

$$(\text{Fc-sp})^{\bullet+}\text{-}C_{60}{}^{\bullet-} \xrightarrow{k_{CR}} \text{Fc-sp-}C_{60} \quad (2)$$

The decay rate constant (k_{CR}) was estimated to be 4.9×10^8 s^{-1}. Thus, the lifetime of the charge-separated state was 2.0 ns.

The longer time-scale phenomena were observed in the nanosecond transient absorption spectra. In Figure 5, a quite small transient absorption band was observed at 700 nm after excitation at 355 nm with the nanosecond laser. The absorption band at 700 nm can be attributed to the triplet excited state of the C_{60} moiety. It should be pointed out that the quantum yield for the triplet generation is smaller than 0.01 for **1** in benzonitrile. The triplet excited state of **1** is considered to be generated via the intersystem crossing process from the singlet excited C_{60} moiety of the dyad, since the triplet state of the C_{60} moiety locates at higher energy level than the charge-separated state as indicated in the schematic energy diagram (Scheme 1). Small quantum yield for the triplet formation accords with the large Φ_{CS} value of the present dyad (0.99).

Generation of the radical ion pair was also confirmed with other dyads, **2** and **3**. In the case of **2** in benzonitrile, the radical cation of the donor moiety appeared around 590 nm after the decay of the singlet excited state of the C_{60} moiety (Figure 6). The peak position of the radical cation of the ferrocene moiety indicates that the linking group has a large contribution to the donor group of the dyad. The rise and the decay rates of the radical cation were estimated to be 4.5×10^{10} and 4.0×10^8 s^{-1}, respectively. The lifetime of the charge-separated state was 2.5 ns. It should be pointed out that the rate constants for the charge separation and recombination of **2** in benzonitrile were slightly faster than **1**, although oxidation and reduction potentials are almost identical (Table 1). The slightly faster rate constants of **1** can be attributed to the fact that the HOMO density of **1**

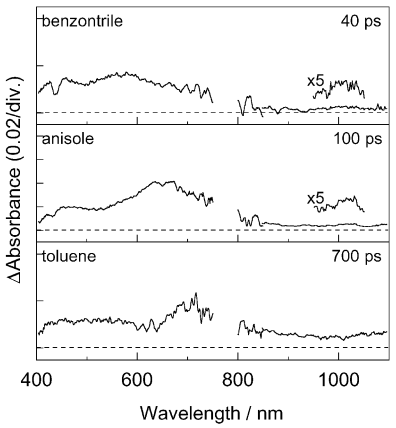

Figure 6. Transient absorption spectra of **2** in benzonitrile, anisole, and toluene upon excitation with the femtosecond laser (388 nm, fwhm 150 fs). Dashed lines indicate ΔAbs = 0.

TABLE 3: Free-Energy Changes of Charge Recombination (ΔG_{CR}), Peak Positions of the Radical Ion Pair (λ_{max}), Charge-Recombination Rates (k_{CR}), and Lifetimes of Radical Ion Pair (τ_{ion}) of Ferrocene−C_{60}-Linked Compounds in Various Solvents

compound	solvent	$-\Delta G_{CR}$/eV[a]	λ_{max}/nm	k_{CR}/s^{-1}	τ_{ion}/ns
1	toluene	1.54	660, 1000	4.9×10^7	20
	anisole	1.20	550, 970	6.2×10^7	16
	benzonitrile	0.88	590, 970	4.9×10^8	2.0
2	toluene	1.57	700, 1020	2.7×10^7	37
	anisole	1.25	640, 1020	3.2×10^7	31
	benzonitrile	0.92	580, 1000	4.0×10^8	2.5
3	toluene	1.78	—[b]	—[b]	—[b]
	anisole	1.17	1000	7.6×10^8	1.3
	benzonitrile	0.96	1000	1.4×10^9	0.7

[a] Estimated by assuming that the ferrocene-ethenyl-phenyl group act as an donor for **1** and **2**. [b] Absorption band due to radical ion pair did not appear clearly.

is located at a spatially closer position to the C_{60}-core than is **2**, indicating that distance for the charge separation in **1** is shorter than in **2**. In the case of **3**, fast charge separation and recombination were also confirmed, as expected from the shorter distance between donor and acceptor moieties of **3**, although the radical cation was not obvious in the transient spectra in the visible region, probably due to localization of the radical cation on the ferrocene moiety. The rate constants for the charge separation and recombination processes were summarized in Tables 2 and 3.

Solvent-Polarity Dependence. In anisole, which is a less polar solvent than benzonitrile, the dyads showed charge separation as in the cases in benzonitrile. In the case of **2** in anisole, the transient absorption band due to singlet excited states of the C_{60} moiety decayed completely at 100 ps after the laser excitation. In the spectrum at 100 ps after the laser, a new absorption band appeared around 640 nm, which can be attributed to the radical cation of the donor moiety of **2**, since the radical anion of the C_{60} moiety was also confirmed around 1000 nm in the transient spectrum (Figure 6). The rate constant for generation of the radical ion pair became smaller in anisole than that in benzonitrile (Table 2). Such a small charge-separation rate in anisole was also confirmed in the fluorescence lifetime measurements as discussed above. Solvent polarity dependence of the charge-separation rates suggests that the charge-separation process belongs to the Marcus "normal region" with reorganization energy (λ) $\geq$ 0.8 eV: Indeed, smaller free-energy changes for the charge separation (ΔG_{CS}) than the λ value were calculated for less polar solvents, as

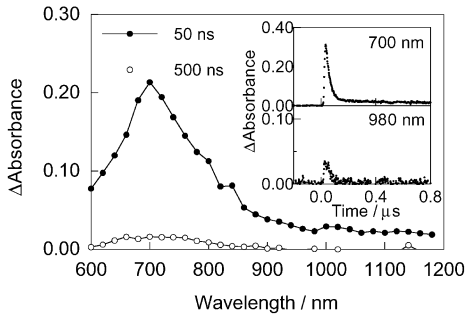

Figure 7. Transient absorption spectra of **2** in toluene upon excitation with the nanosecond laser (355 nm, fwhm 6 ns). Inset: Absorption−time profiles at 700 and 980 nm.

indicated in Table 2. In toluene, further slow charge-separation processes were confirmed for these dyads. It should be noted that the free-energy changes for the charge separation and recombination (ΔG_{CR}) processes of **1** and **2** in Tables 2 and 3 were estimated by assuming that the radical cations are delocalized over the donor groups, i.e., ferrocene-ethenyl-phenyl groups. Assuming that the radical cation is localized on the ferrocene moiety, the energy levels of charge-separated states of **1** and **2** become 0.2 eV higher than the singlet excited state in toluene, which cannot explain the experimental results. This fact will support the consideration that the radical cations are delocalized over the donor groups.

It should be pointed out that the peak position of the radical cation depends on the solvent polarity. The peak positions of the radical cation of **2** in benzonitrile, anisole, and toluene were confirmed at 590, 640, and 700 nm, respectively (Figure 6). The shift of peak position of the radical cation was also confirmed for **1** (Table 3). The large solvent polarity dependence of the peak position possibly indicates that the radical cation moiety is located in close proximity to the radical anion moiety in the charge-separated state of the dyads.

Another possibility for the present spectral shifts depending on the solvent polarity will be the structural change in the charge-separated state. The structural change seems to be possible since the solvent polarity has large effect on the structure of strained π-conjugated bond as known as solvatochromism. For example, compounds with stilbene structure show the structural change of the double bond connecting the phenyl groups in the excited state. In the present dyads, similar structural change is expected for the double bonds connecting the phenyl and ferrocene groups. For **1** and **2**, the MO calculations for the optimized structures (Figure 2) indicated that the ferrocene and phenyl groups are expected to be not in the same plane due to steric hindrance of the phenyl and ferrocene groups. Thus, the introduction of additional charge will cause structural change, which shifts the absorption peak according to the degree of the π-conjugation of the donor moiety. However, isomerization of **1** and **2** seems to be neglected since the steady-state absorption spectra were not changed between the laser experiments. Both close proximity and structural change can explain the fact that the extent of the spectral shift of **2** is larger than that of **1** (Table 3). For **3**, peak position did not depend on solvent polarity due to absence of double bond connecting donor and acceptor.

In less polar solvents, the charge-recombination process could be followed by the absorption bands of the radical ion pair in the nanosecond laser flash photolysis. In the case of **2** in toluene, an absorption band appeared at 700 nm immediately after the nanosecond laser irradiation as indicated in a spectrum at 50 ns in Figure 7. The absorption band that appeared immediately

SCHEME 2

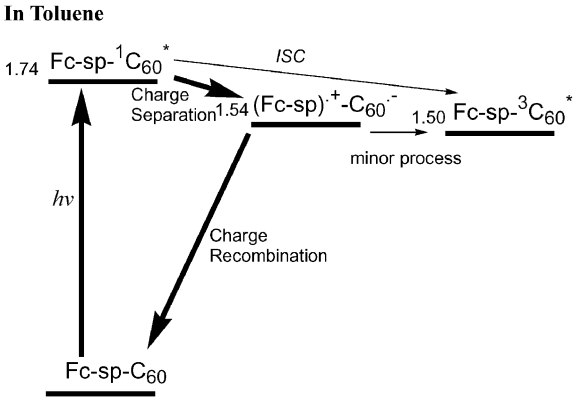

after the nanosecond laser irradiation can be attributed to the radical ion pair, which accords well with the absorption band confirmed in the subpicosecond transient absorption spectrum (Figure 6). The decay rate constant of the radical ions was estimated to be 2.7×10^7 s^{-1}, which corresponds to 37 ns of the lifetime of the radical ion pair of **2**. In anisole, the radical ion pair was also confirmed in the nanosecond transient spectrum, in which the lifetime of the charge-separated state was 31 ns. Thus, the rate constants for charge recombination were in the order of benzonitrile > anisole > toluene. The similar solvent-polarity dependences of the charge-recombination rates were also confirmed for **1** and **3** as listed in Table 3. For charge-recombination processes in less polar solvents, negatively larger free-energy changes were expected as summarized in Table 3. Since the charge-recombination processes are expected to be in the Marcus "inverted region", slow charge-recombination rate constants in less polar solvents are adequate results.

For all the solvents, charge-recombination rate constants were in the order of **2** < **1** < **3**, as pointed out above. This is an adequate trend from the distance between the donor and acceptor moieties, which has a large effect on the lifetimes of the radical ions.

In Figure 7, after decay of the absorption band of the charge-separated state within 100 ns, a small absorption band remained around 700 nm, although the absorption band around 980 nm decayed completely. The remaining absorption band around 700 nm can be assigned to the triplet excited state of the C_{60} moiety, since the absorption band disappeared when the solution was saturated with oxygen, a triplet energy acceptor. Although the generation of the triplet excited states via charge recombination of the charge-separated state is energetically possible for **1** and **2** in toluene (Scheme 2), the contribution of the process seems to be small, since the generation yields of the triplet excited states of **1** and **2** were less than 0.05, which are almost the same as $(1 - \Phi_{CS})$ values. Thus, the intersystem crossing process from the singlet excited C_{60} is concluded to be the predominant pathway for the triplet generation of the present dyads. The low contribution of the charge-recombination process to the triplet formation can be attributed to the smaller driving force, because the energy difference between the charge-separated state and the triplet state was as small as 0.04 eV in toluene, supporting the negligible charge-recombination process yielding the triplet state. In anisole, the energy levels of the charge-separated states of **1** and **2** are lower than the triplet state of the C_{60} moiety, indicating that the triplet excited states of the C_{60} moieties of **1** and **2** are not generated via the charge-recombination processes as in the cases in benzonitrile.

Conclusion

In the present study we showed that novel dyad molecules of ferrocene and fullerene connected with the acetyl-phenyl-ethenyl group indicate the charge-separation and charge-recombination processes, in which the linking groups also participate to the delocalization of the radical cation. These features have not been observed with other ferrocene and fullerene dyads connected with single or double bonds.[7] The large spectral shifts of the absorption bands of the radical cation moieties depending on the solvent polarity are interesting examples indicating the structural change of the dyads in the radical-ion state. The observations of the charge-separation processes in the wide variety of the solvent polarities can be achieved by employment of ferrocene, which makes the ΔG_{CS} values negative even in nonpolar solvents such as toluene. These properties are useful to achieve efficient charge separation in nonpolar environments such as polymer matrices for molecular devices.

Acknowledgment. The present work was partly supported by a Grant-in-Aid on Scientific Research from the Ministry of Education, Science, Sports and Culture of Japan. The authors are also grateful for financial support by Core Research for Evolutional Science and Technology (CREST) of Japan Science and Technology Corporation, and The Mitsubishi Foundation. One of the authors (M.F.) thanks The Kao Foundation For Arts and Sciences for financial support.

Supporting Information Available: The synthetic procedure and spectroscopic and analytical data of **1**−**3** and transient absorption spectra of *N*-methylpyrrolidino C_{60} in toluene. These materials are available free of charge via the Internet at http://pubs.acs.org.

References and Notes

(1) For a review, see: (a) Martin, N.; Sánchez, I.; Illescas, B.; Pérez, I. *Chem. Rev.* **1998**, *98*, 2527. (b) *Fullerenes*, Kadish, K. M.; Ruoff, R. S., Eds. Wiley-Interscience: New York, 2000.

(2) (a) Williams, R. M.; Zwier, J. M.; Verhoeven, J. W. *J. Am. Chem. Soc.* **1995**, *117*, 4093. (b) Williams, R. M.; Koeberg, M.; Lawson, J. M.; An, Y.-Z.; Rubin, Y.; Paddon-Row, M. N.; Verhoeven, J. W. *J. Org. Chem.* **1996**, *61*, 5055. (c) Komamine, S.; Fujitsuka, M.; Ito, O.; Moriwaki, K.; Miyata, T.; Ohno, T. *J. Phys. Chem. A* **2000**, *104*, 11497.

(3) Imahori, H.; Cardoso, S.; Tatman, D.; Lin, S.; Noss, L.; Seely, G. R.; Sereno, L.; Silber, C.; Moore, T. A.; Moore, A. L.; Gust, D. *Photochem. Photobiol.* **1995**, *62*, 1009.

(4) (a) Kuciauskas, D.; Lin, S.; Seely, G. R.; Moore, A. L.; Moore, T. A.; Gust, D.; Drovetskaya, T.; Reed, C. A.; Boyd, P. D. W. *J. Phys. Chem.* **1996**, *100*, 15926. (b) Imahori, H. Hagiwara, K.; Aoki, M.; Akiyama, T.; Taniguchi, S.; Okada, T.; Shirakawa, M.; Sakata, Y. *J. Am. Chem. Soc.* **1996**, *118*, 11771. (c) Imahori, H.; Hagiwara, K.; Akiyama, T.; Aoki, M.; Taniguchi, S.; Okada, T.; Shirakawa, M.; Sakata, Y. *Chem. Phys. Lett.* **1996**, *263*, 545. (d) Imahori, H.; Ozawa, S.; Uchida, K.; Takahashi, M.; Azuma, T.; Ajavakom, A.; Akiyama, T.; Hasegawa, M.; Taniguchi, S.; Okada, T.; Sakata, Y. *Bull. Chem. Soc. Jpn.* **1999**, *72*, 485. (e) Tkachenko, N. V.; Rantala, L.; Tauber, A. Y.; Helaja, J.; Hynninen, P. V.; Lemmetyinen, H. *J. Am. Chem. Soc.* **1999**, *121*, 9378. (f) Schuster, D. I.; Cheng, P.; Wilson, S. R.; Prokhorenko, V.; Katterle, M.; Holzwarth, A. R.; Braslavsky, S. E.; Klihm, G.; Williams, R. M.; Luo, C. *J. Am. Chem. Soc.* **1999**, *121*, 11599. (g) Imahori, H.; El-Khouly, M. E.; Fujitsuka, M.; Ito, O.; Sakata, Y.; Fukuzumi, S.; *J. Phys. Chem. A* **2001**, *105*, 325.

(5) (a) Llacay, J.; Veciana, J.; Vidal-Gancedo, J.; Bourdelnde, J. L.; González-Moreno, R.; Rovira, C. *J. Org. Chem.* **1998**, *63*, 5201. (b) Martin, N.; Sánchez, L.; Herranz, M. A.; Guldi, D. M. *J. Phys. Chem. A* **2000**, *104*, 4648.

(6) (a) Yamashiro, T.; Aso, Y.; Otsubo, T.; Tang, H.; Harima, T.; Yamashita, K. *Chem. Lett.* **1999**, 443. (b) Fujitsuka, M.; Ito, O.; Yamashiro, T.; Aso, Y.; Otsubo, T. *J. Phys. Chem. A* **2000**, *104*, 4876. (c) Fujitsuka, M.; Matsumoto, K.; Ito, O.; Yamashiro, T.; Aso, Y.; Otsubo, T. *Res. Chem.*

Intermed. **2001**, *27*, 73. (d) Hirayama, D.; Yamashiro, T.; Takimiya, K.; Aso, Y.; Otsubo, T.; Norieda, H.; Imahori, H.; Sakata, Y. *Chem. Lett.* **2000**, 570. (e) Fujitsuka, M.; Masuhara, A.; Kasai, H.; Oikawa, H.; Nakanishi, H.; Ito, O.; Yamashiro, T.; Aso, Y.; Otsubo, T. *J. Phys. Chem. B* **2001**, *104*, 9930.

(7) (a) Maggini, M.; Scorrano, G.; Prato, M. *J. Am. Chem. Soc.* **1993**, *115*, 9798. (b) Prato, M.; Maggini, M.; Giacometti, C.; Scorrano, G.; Sandonà, G.; Farnia, G. *Tetrahedron* **1996**, *52*, 5221. (c) Guldi, D. M.; Maggini, M.; Scorrano, G.; Prato, M. *J. Am. Chem. Soc.* **1997**, *119*, 974.

(8) (a) D'Souza, F.; Zandler, M. E.; Smith, P. M.; Deviprasad, G. R.; Arkady, K.; Fujitsuka, M.; Ito, O. *J. Phys. Chem. A* **2002**, *106*, 649. (b) D'Souza, F.; Zandler, M. E.; Smith, P. M.; Deviprasad, G. R.; Arkady, K.; Fujitsuka, M.; Ito, O. *J. Org. Chem.* **2002**, *67*, 9122.

(9) (a) Sariciftci, N. S.; Wudl, F.; Heeger, A. J.; Maggini, M.; Scorrano, G.; Prato, M.; Bourassa, J.; Ford, P. C. *Chem. Phys. Lett.* **1995**, *247*, 510. (b) Maggini, M.; Guldi, D. M.; Mondini, S.; Scorrano, G.; Paolucci, F.; Ceroni, P.; Roffia, S. *Chem. Euro. J.* **1998**, *4*, 1992. (c) Polese, A.; Mondini, S.; Bianco, A.; Toniolo, C.; Scorrano, G.; Guldi, D. M.; Maggini, M. *J. Am. Chem. Soc.* **1999**, *121*, 3446. (d) Guldi, D. M.; Garscia, G. T.; Mattay, J. *J. Phys. Chem. A* **1998**, *102*, 9679. (e) Guldi, D. M. *Chem. Commun.* **2000**, 321. (f) Yamazaki, M.; Araki, Y.; Fujitsuka, M.; Ito, O. *J. Phys. Chem. A* **2001**, *105*, 8615. (g) Guldi, D. M.; Swartz, A. S.; Luo, C.; Gómez, R.; Segura, J. L.; Martín, N. *J. Am. Chem. Soc.* **2002**, *124*, 10875. (h) Fujitsuka, M.; Luo, H.; Murata, Y.; Kato, N.; Ito, O.; Komatsu, K. *Chem. Lett.* **2002**, 968.

(10) (a) Fujitsuka, M.; Ito, O.; Imahori, H.; Yamada, K.; Yamada, H.; Sakata, Y. *Chem. Lett.*, **1999**, 721. (b) Imahori, H.; Tamaki, K.; Guldi, D. M.; Luo, C.; Fujitsuka, M.; Ito, O.; Sakata, Y.; Fukuzumi, S. *J. Am. Chem. Soc.* **2001**, *123*, 2607.

(11) Lamrani, M.; Hamasaki, R.; Mitsuishi, M.; Miyashita, T.; Yamamoto, Y. *Chem. Commun.* **2000**, 1595.

(12) Frisch, M. J.; Trucks, G. W.; Schlegel, H. B.; Scuseria, G. E.; Robb, M. A.; Cheeseman, J. R.; Zakrzewski, V. G..; Montgomery, Jr., J. A.; Stratmann, R. E.; Burant, J. C.; Dapprich, S.; Millam, J. M.; Daniels, A. D.; Kudin, K. N.; Strain, M. C.; Farkas, O.; Tomasi, J.; Barone, V.; Cossi, M.; Cammi, R.; Mennucci, B.; Pomelli, C.; Adamo, C.; Clifford, S.; Ochterski, J.; Petersson, G. A.; Ayala, P. Y.; Cui, Q.; Morokuma, K.; Malick, D. K.; Rabuck, A. D.; Raghavachari, K.; Foresman, J. B.; Cioslowski, J.; Ortiz, J. V.; Baboul, A. G.; Stefanov, B. B.; Liu, G..; Liashenko, A.; Piskorz, P.; Komaromi, I.; Gomperts, R.; Martin, R. L.; Fox, D. J.; Keith, T.; Al-Laham, M. A.; Peng, C. Y.; Nanayakkara, A.; Gonzalez, C.; Challacombe, M.; Gill, P. M. W.; Johnson, B.; Chen, W.; Wong, M. W.; Andres, J. L.; Gonzalez, C.; Head-Gordon, M.; Replogle, E. S.; Pople, J. A. Gaussian 98, Revision A.7, Gaussian, Inc.; Pittsburgh, PA, 1998.

(13) Lee, C.; Yang, W.; Parr, R. G. *Phys. Rev.* **1998**, *B37*, 785.

(14) Luo, C.; Fujitsuka, M.; Watanabe, A.; Ito, O.; Gan, L.; Huang, Y. Huang, C.-H. *J. Chem. Soc., Faraday Trans.* **1998**, *94*, 527.

(15) (a) Arias, F.; Xie, Q.; Wu, Y.; Lu, Q.; Wilson, S. R.; Echegoyen, L. *J. Am. Chem. Soc.* **1994**, *116*, 6388. (b) Arias, F.; Echegoyen, L.; Wilson, S. R.; Lu, Q.; Lu, Q. *J. Am. Chem. Soc.* **1995**, *117*, 1422. (c) Guldi, D. M.; Hungerbühler, H. Asmus, K.-D. *J. Phys. Chem.* **1995**, *99*, 9380.

(16) Ma, B.; Sun, Y.-P. *J. Chem. Soc., Perkin Trans.* **1996**, 2157.